

21 RF sidebands, cavity lengths and control scheme.

There will be two pairs of phase-modulated sidebands, placed on the main beam just downstream of the PSL, in air, using two fast- and high-powered Pockels cells in series. Since these are in series, the second Pockels cell will place sidebands on the first pair of sidebands, producing four desired sidebands at $(\pm f_1, \pm f_2)$ and four “parasitic” sidebands at $(\pm f_1 \pm f_2)$.

The goal is to measure and control the arm degrees of freedom (L_+ and L_-) using beats between the carrier and sidebands, and the power- and signal-recycled Michelson degrees of freedom (l_+ , l_- , and l_s) using beats between sidebands.

The Michelson asymmetry is set to be a bright port for the higher of the two RF sidebands (f_2). The lower RF sideband (f_1) should be as low as possible, so that f_2 “sees” the signal mirror while f_1 does not, providing maximal separation between l_+ and l_s .

Because the 40m cannot accommodate a large power recycling cavity (PRC) (it is limited by the vacuum envelope to be on the order of 2 meters), we will see that the 40m cannot make use of values for f_1 as low as that proposed for LIGO II (9 MHz); thus, the ratio f_1/f_2 will be larger at the 40m than at LIGO and the separation between l_+ and l_s will be worse. If we can make this work at the 40m, it will only be easier at LIGO (I think).

Both pairs of sidebands will be placed on the beam before the input mode cleaner. The mode cleaner must pass both pairs of sidebands, so their frequencies must be chosen to be multiples of the FSR of the mode cleaner.

The input mode cleaner will have a half-length of approximately $L_{MC} = 12.69$ m, determined by the length of the 8” diameter and 12 m long MC pipe, and the positions of the suspensions in the chambers on either end of the pipe. Then, $FSR_{MC} = c/2L_{MC} = 11.82$ MHz. For a triangular mode cleaner, it’s the *half*-length, and not the total length, which determines the FSR (for a linear Fabry-Perot cavity, the round-trip length is twice the total length; for a triangular Fabry-Perot, the total round trip length is twice the half length).

The f_1 sidebands must resonate in the MC, so they must be an integral multiple of FSR_{MC} . In addition, they must resonate in the PRC. Recall that the carrier sees an overcoupled arm reflectivity whose sign is opposite to that of the sidebands. Thus, if the carrier is resonant in the PRC, the sidebands must experience an additional phase shift of $(2n + 1)\pi$, where n is some integer. Thus, we require $f_1 = (2n + 1)c/(4L_{PRC})$. The length of the PRC can be made as short as 2 m or as long as 2.5 m or maybe even longer. We want f_1 to be as small as possible (see above), so we choose $n = 0$ and thus $f_1 = c/(4L_{PRC})$. The smallest multiple of FSR_{MC} that can satisfy this is $f_1 = 3FSR_{MC} = 35.46$ MHz, with $L_{PRC} = c/(4f_1) = 2.115$ m.

Now we want the second pair of sidebands (f_2) to be as high as possible, and resonant in the MC and in the PRC; so it should be a multiple of f_1 . We can choose $f_2 = 5f_1 = 15FSR_{MC} = 177.3$ MHz. This is close to the 180 MHz chosen for LIGO II. It’s about as high as one dares to go using present photodetector, mixer, and RF distribution technology.

As we will see below, the mixer will need to demodulate at $f_2 \pm f_1$; at LIGO II, this is $180+9 = 189$ MHz; but at the 40m, this is 212.8 MHz. Too high? Actually, the current scheme calls for *double-demodulation*; instead of demodulating at $f_2 + f_1$ and at $f_2 - f_1$, one can demodulate at f_2 , and then feed the output to a mixer demodulating at f_1 ; this accomplishes the same thing. So we’ll only need to demodulate at 177.3 MHz at the 40m.

Now we choose the Michelson asymmetry to make the asymmetric port of the BS “bright” for the f_2 sidebands, so that the f_2 sidebands “see” the signal recycling mirror. We need a Michelson asymmetry of $|\delta l| = c/(4f_2) = 0.423$ m, or Michelson arm lengths that differ by ± 0.211 m. This

should be easy to arrange in the 40m vacuum envelope.

Of course, some of the f_1 sidebands will also go out the asymmetric port of the BS. Because f_1/f_2 must be larger at the 40m than at LIGO, more f_1 sideband will go out the asymmetric port, degrading the separation between the sensing of the l_+ and l_s degrees of freedom. The fraction of f_1 sideband power exiting the asymmetric port of the BS is small but non-zero (about 10%).

Finally, we must determine the length of the signal recycling cavity (SRC). If we put the signal recycling mirror in the same chamber as the BS and PRM, then we want the SRC to be roughly the same length as the PRC, or only a tiny bit larger (not smaller!). If we put the SRM in the output optic chamber, then L_{SRC} must be between 0.8xx and 1.5xx meters longer than L_{PRC} . We want the f_2 sidebands to be resonant in the SRC.

However, the carrier light will be detuned in the SRC; not resonant. Choosing a round-trip detuning of $d\nu = 0.25$ (in units of 2π) for the carrier light will produce a dip in the shot-noise curve for the GW signal, at ~ 1500 Hz. We can make the f_2 sidebands resonant in the SRC, if $L_{SRC} = (2 + d\nu + 1/2)(c/2f_2) = 2.3265$ m, or 21 cm longer than L_{PRC} . This can be accomodated in the BS chamber.

All these cavity lengths are *optical* path lengths; physical distances will be a bit smaller due to light travelling through glass.

Parasitic frequencies exist at $\pm f_2 \pm f_1 = \pm 141.8$ MHz and ± 212.8 MHz. Peter Fritchel and Ken Strain say that they're not a problem, which I find hard to believe; a Twiddle study to verify this is in progress. XXX

Table 1 summarizes all the frequencies and lengths. They satisfy the following resonant conditions:

$$\begin{aligned}
 f_2 &= qf_1, & q &= 5; \\
 L_{MC} &= n\frac{c}{2f_1}, & n &= 3; \\
 L_{PRC} &= (k + 1/2)\frac{c}{2f_1}, & k &= 0; \\
 L_{SRC} &= (p + d\nu + 1/2)\frac{c}{2f_2}, & p &= 2, \quad d\nu = 0.25; \\
 L_{SRC} &= (\mu + 1/2)\frac{c}{2f_1}, & \mu &= (p + d\nu + 1/2)/q - 1/2 = 0.1 \neq \text{integer}; \\
 L_{ARM} &= (m + 1/2)\frac{c}{2f_1}, & m &= 8.5425.
 \end{aligned}$$

OK, the last one is far from the desired resonant condition. The limited range over which we can change L_{ARM} and L_{MC} at the 40m means that we can't quite keep the sidebands at or near antiresonance in the arms, and thus there's non-negligible sideband light in the arms. We'd need to make the arms a couple of meters longer, or the mode cleaner more than 50 cm shorter, to get to antiresonance. But, the arms are high-finesse cavities; even far from anti-resonance, the sideband light power in the arms is not high. Although the presence of sideband light in the arms degrades the LSC control matrix diagonality somewhat, it's tolerable; and I know of no other ill effects that this causes.

Finally, in order to implement DC detection of the GW signal, we need to let a little bit of carrier light out the dark port. This can be done either by slightly offsetting the arms from exact resonance (in opposite directions in the two arms), or by offsetting the Michelson asymmetry. It is believed that the former is better, since the light so leaked has been filtered by the arms. Arm

Table 1: Phase-modulated sideband frequencies, and optical path lengths of resonant cavities.

f_{srmc} (MHz)	11.82
$f_1 = 3f_{srMC}$ (MHz)	35.46
$f_2 = 15f_{srMC}$ (MHz)	177.30
L_{MC} (m)	12.69
L_{PRC} (m)	2.115
L_{SRC} (m)	2.326
Δl_{PRC} (m)	0.423
L (BS-ITMinline) (m)	2.1115
L (BS-ITMperp) (m)	1.6885
L (BS-PRM) (m)	0.215
L (BS-SRM) (m)	0.426

offsets at the level of $\pm 5 \times 10^{-12}$ m will let a bit of carrier light out the dark port (1.3 mW for an input power of 1 watt), making little change to the fields anywhere else. No other changes are required to the optical configuration or controls, as far as I can tell...

21.1 Twiddle Model

A Twiddle [18] model has been used to verify the resonance conditions described above (Table 2), determine the DC fields at all points (Table 3), predict the DC response at the photodetectors to all length changes (and thus the LSC control matrix) (Table 4), and predict the shape of the GW response function (Fig 21.1).

Because of the signal cavity detuning, the sideband fields everywhere in the IFO are asymmetric (different power for $+f_1$ dieband than for $-f_1$, and similarly for $\pm f_2$). Only one sideband in a pair is useful for length sensing. The consequent loss in length sensing sensitivity is compensated for by the increased sensitivity in the shot noise dip region. And, it has no effect on the GW DC readout sensitivity.

In these tables and figures, there is no arm DC offset, so no carrier light leaks out the dark port for DC detection. The addition of a small, balanced arm DC offset makes little change to anything except the amount of carrier light exiting the dark port.

These numbers are NOT final! Several things have not yet been optimized:

- There's sideband light in the arms, because the sidebands are not near antiresonance. We need to find out how much we can push the ratio L_{ARM}/L_{MC} towards the nearest resonant condition, given the vacuum envelope. This will improve the LSC matrix diagonality.
- We need to optimize the modulation depths, the pickoff reflectivity, and (what else? XXX).
- we may want to optimize T_{SRM} , and even T_{PRM} .
- We need to update all the numbers in the following section.

Table 2: Various quantities characterizing the DC response of the 40m optics, (no arm offset).

T(ITM)	0.005
T(RM)	0.086
T(SM)	0.086
SRC carrier roundtrip tune	0.252π
Arm cavity carrier finesse	1231
PRC carrier finesse	38
Arm cavity carrier power gain	770
PRC carrier power gain	14
Sym Port carrier power reflectivity	0.01

Table 3: DC power in the 40m cavities (no arm offset). The signal cavity detuning produces an asymmetric response for the sideband pairs, thus, effectively, only one sideband is used for generating error signals.

frequency	$-f_2$	$-f_1$	carrier	f_1	f_2
Modulation depth Γ	0.1	0.1		0.1	0.1
Input from Laser	0.00249	0.00249	0.99003	0.00249	0.00249
Reflected (SP)	0.00001	0.00227	0.01005	0.00211	0.00249
Asym port (AP)	0.00239	0.00015	0.00000	0.00030	0.00000
PR Cavity	0.02788	0.04186	13.8354	0.04693	0.00006
SR Cavity	0.02544	0.00154	0.00000	0.00315	0.00005
Arm Cavity	0.00009	0.00188	5323.0	0.00104	0.00000

Table 4: LSC signals. \otimes means double demodulation.

Signal	L_+	L_-	l_+	l_-	l_s
SP, f_1	-304	0.000	0.353	0.004	0.003
AP, f_2	0	-57.7	0	-0.072	0
SP, $f_2 \otimes f_1$	-0.007	-0.001	0.136	-0.009	-0.053
AP, $f_2 \otimes f_1$	-0.005	-0.017	0.043	-0.246	0.007
PO, $f_2 \otimes f_1$	-0.045	-0.006	0.089	0.081	-0.722

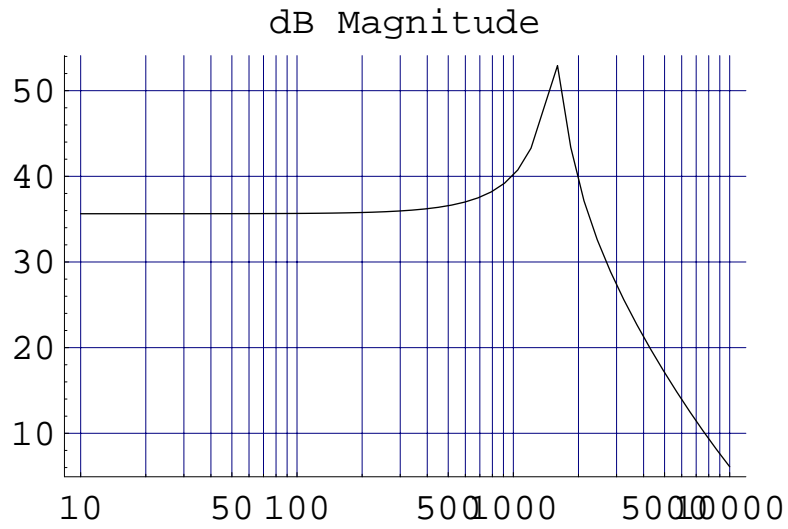


Figure 1: GW (L_-) response for 40m parameters, as predicted by Twiddle. The choice of signal cavity roundtrip detune of 0.5π produces a peak in the response, and a dip in the shot noise sensitivity, at around 1500 Hz.

22 Suspended optical components

The 40m prototype upgrade will (initially) contain three suspended optics for the 12m mode cleaner, and 7 core optics (PRM, SRM, BS, two ITMs, and two ETMs).

We may need to develop a suspended monolithic output mode cleaner. Other in-vacuum optics, including the mode matching telescope and steering mirrors (which are suspended in LIGO I) will be fixed on the optical tables at the 40m. This is primarily due to lack of in-vacuum real estate for suspensions. We can get away with it because there is low priority for “heroic” efforts to reduce noise from these sources in the GW signal.

With the optical configuration to be described below, the beam is everywhere (from the 12m mode cleaner on) on the order of $w_0 \sim \sqrt{\lambda L_{arm}/\pi} \sim 4.0$ mm in transverse dimension (amplitude $1/e$ radius). This corresponds to a power $1/e$ radius of $r_0 = w_0/\sqrt{2} \sim 2.8$ mm, power $1/e^2$ diameter of $d_{1/e^2} = 2\sqrt{2}w_0 \sim 11$ mm, and power 1ppm diameter of $d_{1ppm} \approx 11w_0/\sqrt{2} \sim 31$ mm.

Because of the inevitable misalignments, and to play it safe, we require 50 mm clear aperture for all optics except for the beam splitter, where we require a factor $1/\sin(45^\circ) = 1.4$ larger clear aperture (in the horizontal direction).

OSEM sensor/actuators have an outer diameter of 25 mm and are centered 3 mm radially from the edge of the optic. Consequently to ensure a 50 mm clear aperture, the optic must be at least 75 mm in diameter (3”). The beam splitter (and MC flat mirrors) are at 45° to the beam, but the OSEMs for these optics can be placed further to the top and bottom of the optic, ensuring maximal clear aperture in the horizontal dimension. This is probably sufficient for all optics except for the test masses (ITMs and ETMs), as discussed below.

LIGO I input suspended optics [19] (mode cleaner and mode matching telescope) use 3” diameter, 1” thick (more precisely, 78mm diameter, 28mm thick), on SOS suspensions [20]. These optics and suspensions are fully engineered and relatively well understood; some 20 of them have been built for LIGO I. They appear to be entirely appropriate for use in the 40m prototype upgrade, for the 12m mode cleaner and for the PRM, SRM, and BS.

22.1 Choice of test mass optic size and aspect ratio

The four test mass optics (ITMs and ETMs) contribute thermal noise to the GW signal. As discussed below, this test mass thermal noise will likely dominate the entire GW noise spectrum above 100 Hz; therefore, some effort should be made to minimize it.

Thermal noise in the GW channel is generically of the form

$$S_x^{thermal} \sim \left(\frac{\tilde{h}L}{2}\right)^2 = \frac{4k_B T}{m\omega} \sum_n \left[\frac{\alpha_n \omega_n^2 \phi_n(\omega)}{(\omega_n^2 - \omega^2)^2 + \omega_n^2 \phi_n^2} \right]$$

where S_x is the displacement noise power spectrum, \tilde{h} is the equivalent GW noise power spectrum, k_B is Boltzmann’s constant, T is the temperature, $\omega = 2\pi f$ is the GW frequency, m is the mass of the test mass, and the sum is over normal modes of vibration with resonant frequency $\omega_n = 2\pi f_n$, effective mass [11] α_n , and loss angle ϕ_n .

There are two sources of thermal noise that are relevant here: suspension thermal noise (pendulum and wire violin modes), and internal test mass thermal vibrations.

Suspension thermal noise in \tilde{h} scales like $1/\sqrt{m}$, so larger masses reduce this. The pendulum thermal noise peaks at the pendulum frequency of $f_0 = 1$ Hz and falls like $1/f^{3/2}$. Above 100 Hz, it is negligible at the 40m (see noise discussion below). The wire violin modes have resonances that

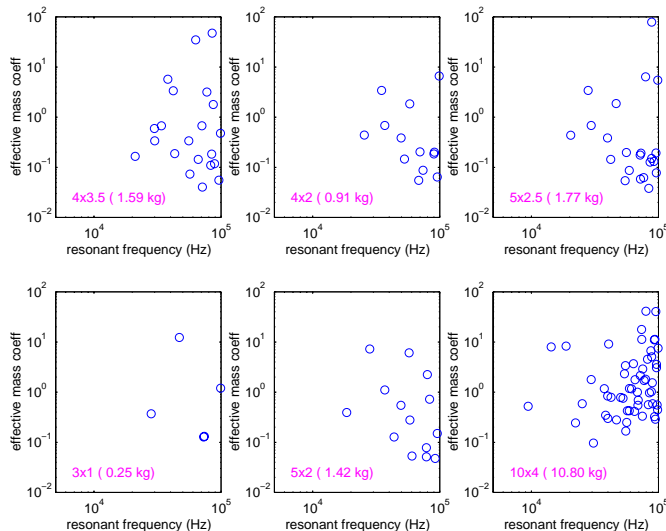


Figure 2: frequencies and effective masses of the node 0 (drumhead and breathing) modes of a right-circular cylinder of the dimensions shown [11].

are right in the detection band, and they have very high $Q = 1/\phi_n(\omega_n)$. Although they may have some impact on a GW signal search, they are not a problem for the 40m program. The noise lines at discrete frequencies in the GW channel may even serve as a useful sign-post in diagnosing the IFO. Nonetheless, they can be minimized by choosing a large mass.

The test masses have natural resonant frequencies which, for the optic sizes we are considering (much smaller than LIGO), are well beyond the Nyquist frequency of our 16kHz ADCs. The frequencies and effective masses of the node 0 (drumhead and breathing) modes, calculated with `testmass5.c` [11], are shown in Fig. 22.1.

These internal resonances have high Q and thus leak only a little into the GW frequency band via dissipation, at a level $\tilde{h} \sim \phi_n$. We thus want to minimize the loss ϕ_n . How does this scale with test mass size and aspect ratio?

The intrinsic loss of fused silica should depend only on the anelastic property of the material, and thus is not expected to scale with mass. This loss is very small, on the order of 10^{-7} ; this is a primary reason why fused silica is the material of choice for LIGO I (and why sapphire may be even better for Advanced LIGO).

Our test masses will have attachments (standoffs) for the suspension wires and the actuator magnets. These provide a loss mechanism which dominates the total loss in our test masses. The loss is given by

$$\phi(f) \sim \frac{dU/dt}{2\pi fU}$$

where U is the total energy stored in the optic. The attachments present a “hole” for energy leakage, proportional to the area A of the attachment on the test mass surface and to a “coupling” κ which depends on the “softness” of the attachment, the position of the attachment relative to the spatially varying vibrational mode, *etc.*. With an energy density u and volume V , $U = uV$, and $dU/dt \sim \kappa uA$, so that $\phi(f) \sim \kappa A/V$. Assuming the attachment area is fixed, independent of test mass size, this suggests that larger masses have less loss due to attachments; as this loss dominates, we can minimize thermal noise by maximizing the test mass size.

For intrinsic loss, it is assumed that κ grows linearly with f , so that $\phi(f) = 1/Q(f)$ is independent of frequency. For attachment loss, we might assume κ is roughly independent of frequency.

What about aspect ratio (optic radius to thickness)? The thinner the optic, the less beam loss due to absorption and scatter. But it also leads to lower-frequency vibrational modes (saddle and drum-head), which may come close to the GW signal and IFO control frequency bands. This was of some concern for the rather thin LIGO beam splitter [12], and it presumably played a role in determining the optimal aspect ratio for the LIGO core optics [13]. This is not a concern for the small optics used at the 40m.

In [14], it is shown that the internal thermal noise is a weak function of aspect ratio, with thicker optics preferred. It's a very weak function, however; and internal thermal noise does not dominate for us.

Stan Whitcomb [15] has suggested that the LIGO aspect ratio (10" diameter, 4" thick) "may reduce undesirable parasitic torques from sideways forces on the magnets".

There are also practical matters to consider, such as price and availability of the optic blanks, polishing, hanging and balancing. However, these don't seem to be significant in driving a decision [16].

We can have relatively large mass and "understood" (ie, LIGO I) aspect ratio, by choosing test masses with 5" diameter, 2" thickness. This gives 1.4 kg test masses. They can be purchased, polished, and coated with acceptable cost and schedule, and can be hung on a straightforwardly-scaled up LIGO SOS suspension [16]. This is what we choose, for the two ITMs and two ETMs.

22.2 Specifications for suspended optics

Specifications must be established for the the suspended optics mirror blank material, polishing, and coating.

Specification details and drawings are in the 40m COC web page [17]. Here we summarize. Mirror blank material specifications:

- Dimensions for the two MC flat mirrors, the MC curved mirror, the PRM, SRM, and BS: 78_{-0}^{+1} mm diameter, 28_{-0}^{+1} mm thickness.
- Dimensions for the four test masses: 125_{-0}^{+1} mm diameter, 50_{-0}^{+1} mm thickness.
- Clear aperture: central 50 mm for all optics except for the BS and the two MC flat mirrors, which are 70 mm.
- Material: fused silica. For the BS and ITMs, through which significant power passes, we choose low-absorption Heraeus SV glass (< 1 ppm/cm absorption). For all the other optics, we can live with < 20 ppm/cm absorption, as achievable with Corning glass.
- Limits on defects, homogeneity, absorption, birefringence, bubbles and inclusions.

Mirror polishing specifications:

- Sides and bevels polished to transparency.
- Limits on number and size of scratches and point defects.
- Surfaces are nominally flat or spherical concave. Concave surfaces have specified radius of curvature (see below) with tolerances, and a limit on astigmatism (typically: ≤ 10 nm).

- Surface errors are specified as a limit on rms deviation from the best fit spherical surface, as measured from phase maps.
 - Low spatial frequency ($\leq 4.3 \text{ cm}^{-1}$) contributing to small angle scattering: typically $\sigma \leq 0.8 \text{ nm}$.
 - High spatial frequency ($4.3\text{--}7,500 \text{ cm}^{-1}$) contributing to large angle scattering: typically $\sigma \leq 0.1 \text{ nm}$. This corresponds to “super-polish”.

These specs require detailed modeling to establish. These studies are in progress (Ganezer for FFT, and Mike Smith for scattering noise). While we wait, it is best to specify the best performance that can be achieved with established techniques, which are good enough for LIGO; hence, the “typical” numbers given above.

- Wedge angles. These have been specified by Mike Smith, to provide adequate separation of secondary beams for pick-offs and baffling (all in the horizontal plane). His estimates, as of 8/25/00: RM: 2.5 deg; BS: 1.0 deg; ITM: 1.0 deg; ETM: 2.5 deg; SM: 2.5 deg.

Mirror coating specs:

- Coatings are for $\lambda = 1064 \text{ nm}$.
- Angle of incidence to be 0° for the PRM, SRM, ITMs, ETMs, and MCcurved; 45° for the BS and two flat MC mirrors.
- Surface 1 (high-reflectivity): specified power transmission (see below).
- Surface 2 (anti-reflection coating): reflection of $(600 \pm 100) \text{ ppm}$.
- limits on non-uniformity, scatter, and absorption.

22.3 Radii of curvature

We can make the cavity symmetric (ITM and ETM with equal curvature, beam waist half-way between), half-symmetric (ITM flat, ETM curved, beam waist at ITM), or somewhere in between (The LIGO I beam waist is a bit closer to the ETM, in order to keep the spot size at the ETM below some limit).

There are no compelling arguments for any choice, here. However, choosing a flat ITM means: (a) placing the waist at the ITM means that one can directly measure it with the ITM camera; (b) the beam is a bit smaller in the input optics than it might otherwise be; (c) it might be faster to get a nominally flat replacement optic, if necessary.

We therefore choose half-symmetric arm cavities, with flat ITMs.

We choose an arm cavity g-factor (see Appendix) of $1/3$, for optimal stability. The arm cavities will be of equal length; nominally, 38.25 m. Therefore, the ROC of the ETM shall be 57.375 m. It is reasonable to expect a few percent tolerance on this number from the polishing process. However, we must require that the two ETMs have the same ROC to 1% (see Appendix).

The beams from the arms propagate through the 50 mm thick ITM (with $n = 1.4496$), then through an *average* of 1.80 meters to the beam splitter. In the current design of the readout scheme, the PRM is 200 mm from the BS, and the SRM is 450 mm from the BS. This determines the beam spot sizes and ROC of all the core optics, as specified in Table 5.

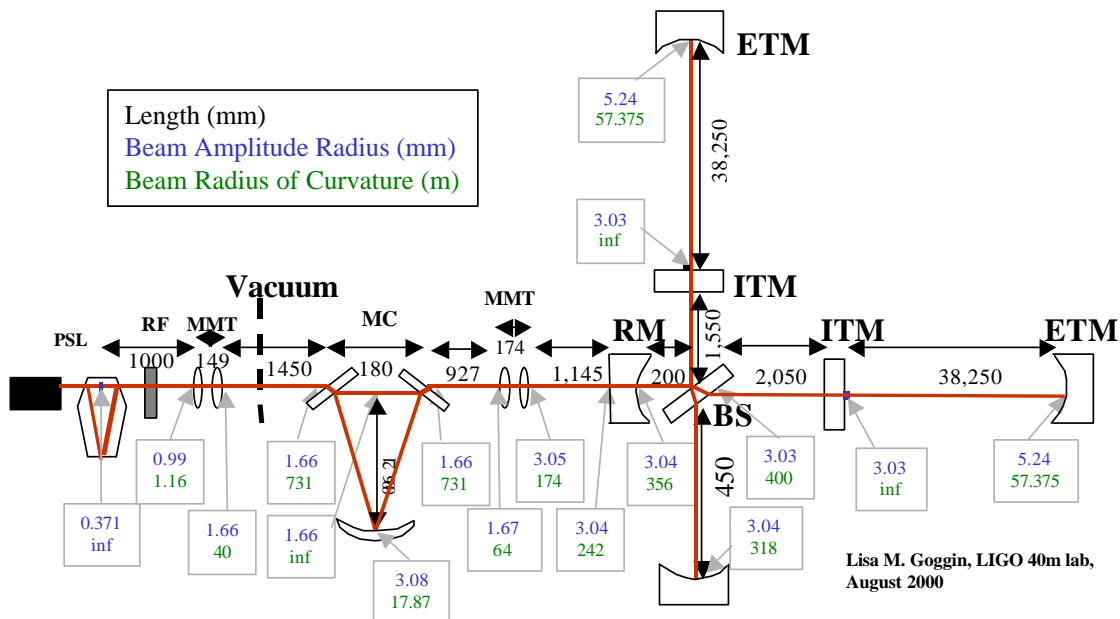


Figure 3: Cavity lengths, beam widths, and ROC at all optics for the 40m prototype upgrade.

In each case, we determine tolerances on the ROC by requiring that the incoming beam be mode-matched to the arm cavity beam, with higher order mode loss of 1%. Details are in the Appendix.

22.4 Mode Cleaner optics

For now, the mode cleaner configuration is planned to be a duplicate of the LIGO I 4K version [19].

The cavity length will be a bit longer (12.246m for LIGO 4K, 12.690m for the 40m). We keep the same g-factor of 0.29, so the ROC of the curved mirror (MC2) goes from 17.25m to 17.87 m, with roughly 2% tolerances. We keep the same mirror dimensions, materials, polishing, and transmittances. These are as summarized in Table 5.

22.5 Coatings

As discussed above, we endeavor to make the 40m optical configuration as close as possible to what is planned for Advanced LIGO (mirror transmissions, cavity finesse; *not* arm cavity storage time!). Currently, the numbers are as summarized in Table 5 and Fig. 22.5.

23 Appendix

For a linear Fabry-Perot optical cavity of length L , such as the IFO arms, we define [21, 22] a g-factor $g = g_1 g_2$, where $g_i = 1 - L/R_i$, $i = 1$ or 2 for the ITM or ETM, respectively, and R_i is the ROC of mirror i . Cavities with $g < 1$ are stable. Furthermore, it can be shown that with beam spot sizes w_i at the two mirrors, the value of $\sqrt{w_1^2 + w_2^2}$ is minimized with $g = 1/3$. We refer to this as optimal stability, and choose this value for the 40m arm cavities (as for the LIGO cavities).

Table 5: Preliminary mirror parameters for the 40m prototype upgrade.

Mirror	diameter (mm)	thickness (mm)	mass (kg)	wedge (deg)	ROC (m)	spot w (mm)	power T
PRM	78	28	0.30	2.5	356	3.04	$(8.6 \pm 0.8)\%$
SRM	78	28	0.30	2.5	318	3.04	$(8.6 \pm 0.8)\%$
BS	78	28	0.30	1.0	∞	3.03	50.0%
ITMs	125	50	1.35	1.0	∞	3.03	$(0.5 \pm 0.05)\%$
ETMs	125	50	1.35	2.5	57.4	5.24	15ppm
MC1, MC3	78	28	0.30	0	∞	1.66	$0.2\% \pm 100$ ppm
MC2	78	28	0.30	0	17.3	3.08	10ppm

For a symmetric cavity, we specify $g_1 = g_2 = \sqrt{g}$, while for a half-symmetric cavity, we specify $g_1 = 1$ (flat ITM) and $g_2 = g$.

The beam waist in such a cavity (field amplitude $1/e$ radius) is determined from the standard formulas:

$$w_0^2 = \frac{\lambda}{\pi} \frac{\sqrt{L(R_1 - L)(R_2 - L)(R_1 + R_2 - L)}}{R_1 + R_2 - 2L}.$$

Here, $\lambda = 1064$ nm.

The Rayleigh length of the beam is

$$z_R = \pi w_0^2 / \lambda.$$

For a half-symmetric cavity, this reduces to

$$w_0^2 = \frac{\lambda L}{\pi} \sqrt{\frac{g}{1-g}}, \quad \text{and} \quad z_R = L \sqrt{\frac{g}{1-g}}.$$

The distance of the waist to mirror 1 (the ITM) is

$$z_i = L(R_2 - L)/(R_1 + R_2 - 2L).$$

The width of the beam (field amplitude $1/e$ radius) at a distance z from the waist is

$$w(z) = w_0 \sqrt{1 + (z/z_R)^2}$$

and the radius of the beam wavefront there (which should match the ROC of a focussing optic, if any, there) is

$$R(z) = z + z_R^2/z.$$

Note that at the waist, $R(0) = \infty$, and $w(0) = w_0$ is minimized. Far from the waist ($z \gg z_R$, ie, the geometrical optic limit), $R = z$ and $w = (w_0/z_R)z$. The power $1/e^2$ diameter is $d_{1/e^2} = 2\sqrt{2}w$, so that the beam divergence full-angle is

$$\theta = 2\sqrt{2}(w_0/z_R) = 2\sqrt{2}\lambda/(\pi w_0).$$

These equations define the beam in the F-P cavity. For LIGO-like IFOs, the arm cavities *define* the TEM₀₀ mode of the beam, and all upstream optics must match efficiently into the arms. Thus, one must propagate the beam in the arms upstream, determine the beam wavefront radius at the

location of each optic, and choose that to be the ROC of the optic placed in that location (except for the BS, which is not a F-P focussing element).

We can use the above formulas to propagate the beam upstream, taking into account the focussing of the curved optics and the different optical path length through fused silica. It is easier, however, to do this using the complex beam parameter $q(z)$, where [22]

$$\frac{1}{q(z)} = \frac{1}{R(z)} - \frac{i\lambda}{\pi w^2(z)}.$$

This beam parameter can be propagated through empty space: $q(z_2) = q(z_1) + (z_2 - z_1)$; through a substrate of thickness t and index of refraction n : $q(z_2) = q(z_1) + t/n$; and through a thin focussing element (like a mirror surface of ROC R): $1/q(z_2) = 1/q(z_1) - 1/R$.

At any point, the beam parameters may be determined:

$$R(z) = \frac{1}{\text{Re}(1/q)}, \quad \text{and} \quad w(z) = \sqrt{\frac{-\lambda}{\pi \text{Im}(1/q)}}.$$

Optimal mode matching then requires any focussing optic placed at that point to have a $ROC = R(z)$.

Also at any point, the beam waist w_0 , and distance to the waist z_w , may be determined:

$$z_w = \text{Re}(q), \quad \text{and} \quad w_0 = \sqrt{\frac{-\lambda}{\pi \text{Im}(1/(q - z_w))}}.$$

Imperfect ROC for, eg, the recycling mirror will produce a beam that is not matched to the one defined by the arms (“mode mismatch”, MM). If this mismatch is small, and approximate expression for the fraction of power lost to higher order modes is [23]

$$MM = \left(\frac{w_0 - w_a}{w_a}\right)^2 + \left(\frac{z_w - z_a}{2z_R}\right)^2,$$

where w_0 is the beam waist of the incoming beam after passing through the imperfect optic, w_a is the waist of the beam defined in the arms, z_w is the distance to the waist for the incoming beam after passing through the imperfect optic, z_a is the distance to the waist of the beam defined in the arms, and z_R is the Rayleigh length of the beam defined in the arms. We want to keep $MM < 0.01$ everywhere.

A simple matlab program has been used to accomplish this propagation, and to evaluate the tolerances on the mirror ROC to keep $MM < 0.01$. They yield the numbers given in Table 5.

24 Suspensions

In the first incarnation of the upgraded 40m ifo, we will focus on the control of the dual-recycled optical configuration. Learning how to control prototypes of advanced (multiple pendulum) suspensions at the same time will be difficult, so we choose to start with LIGO I-like single pendulum suspensions, which will have been well characterized and understood within the coming year.

Following this, we *may* choose to implement (scaled-down) prototypes of multiple pendula, if the overall goals of the Advanced LIGO R&D work calls for it. Full scale Advanced LIGO multiple pendulum suspensions cannot be accommodated in the 40m vacuum chambers; these will be tested at the LASTI facility at MIT.

24.1 Suspension mechanical

We will need two types of mechanical suspensions for the 40m upgrade, to support the two sizes of optics we will be using (3"x1" and 5"x2"). The 3"x1" suspensions can be exact replicas of the SOS suspensions currently in use at LIGO for the mode cleaner and mode-matching telescope [20], with modifications to reflect lessons learned during LIGO I commissioning (if any; at present, we know of none).

The 5"x2" suspensions can be simply scaled-up versions of the existing SOS suspensions. They can be designed so that the various resonant frequencies are identical to that of the LIGO SOS suspension (why might we want to do that? XXXX):

- The pendulum frequency shall be 1.0 Hz (controlled by the length from the suspension block on top to the center of the optic, $d_{pend} = 248$ mm);
- the pitch frequency shall be 0.75 Hz (controlled by the distance the wire standoff is above the optical center line of the optic, $d_{pitch} = 0.277$ mm);
- the yaw frequency shall be 0.85 Hz (controlled by the distance between the wires on the suspension block, $d_{yaw} = 27.5$ mm).

The 3"x1" SOS suspensions have dimensions of 417 mm (height), 155 mm (transverse width), 127 mm (longitudinal width). The center of the suspended optic is 139.7 mm from the bottom of the support structure.

The 5"x2" SOS suspensions have dimensions of 425 mm (height), 241 mm (transverse width), 165 mm (longitudinal width). The center of the suspended optic is 139.7 mm from the bottom of the support structure.

The suspension cages are made of stainless steel and aluminum. The wire, suspension block, wire standoffs, magnets and standoffs, sensor/actuator heads and head holders, safety cage and safety stops, and cables and cable harnesses, would be as described in [20].

(Mods for the OSEMs, to shield stray light? Anything else? xxx)

24.2 Suspension control

The LIGO I suspension controls are currently being redesigned to provide RF modulation of the LED/PD sensor (to reduce the effect of stray 1064 light entering the sensor), and to provide digital control and filtering of the velocity damping functions. These newly designed control electronics elements would be replicated for the initial 40m upgrade.

25 Optical parameters of the Interferometer

25.1 arm optical parameters

The LIGO-like IFO configuration is a power-recycled Michelson IFO with Fabry-Perot arms (PRM-FP), with no "signal" mirror (SM) in the dark port.